

## Investigation of the Magnetic Properties of an RF-Driven Inductively Coupled Argon Plasma

O. VOZNIY,\* M. VORONKO, B. J. PARK and G. Y. YEOM

*Department of Materials Science & Engineering, Sungkyunkwan University, Suwon 440-746*

(Received 29 March 2006, in final form 14 August 2006)

The magnetic permeability of an inductively coupled argon radio-frequency plasma was investigated under the local influence of a magnetizing coil, which additionally served as a probe. During the transition from one steady state to another, the electric current through the measuring transformer, as well as the value of the magnetic permeability of the medium, was shown to change. The latter strongly depended on the primary coil's magnetizing current and on the voltage generated at the ends of the secondary coil until permeability saturation occurred. The magnetic permeability, the magnetic inductance, and the field were estimated as functions of the induced power.

PACS numbers: 52.70.Ds

Keywords: Magnetic permeability, Inductively coupled plasma, Magnetizing coil, Vector diagram

### I. INTRODUCTION

Sources of inductively coupled plasmas (ICP) are widely used in modern technology at pressures ranging from  $10^{-4}$  Torr up to atmospheric absolute pressure. The process of plasma generation is based on the phenomenon of resonance in oscillating circuits. In spite of simple engineering design of the sources and the matching units [1], the question of effective power transmission to the discharge region remains poorly explored.

Charge distribution inside an ion source volume, as well as the electromagnetic fields generated by a planar or solenoid-type antenna, can be described on the basis of Maxwell equations by introducing the concept of the skin depth [2]. The depth represents the distance at which power from the source can be effectively transferred to the discharge region by means of an electromagnetic interaction. For a solenoid-type antenna the peak of the ion concentration in the radial direction is observed at a distance determined by the penetration of the electromagnetic field into the plasma and by the thickness of the dielectric window. Due to the relatively high mobility and concentration, such peaks for the electron concentration and the energy distribution were not found [3].

At present, a new approach based on an equivalent electric circuit description is proposed to illuminate the nature of ICP discharge phenomena [4,5]. By using the

parameters of the equivalent circuit of an oscillating loop and the magnitudes of its components, one can determine the value of the antenna impedance. The latter includes both real and imaginary components. This fact leads to a possibility to describe the antenna properties in terms of an inductance coil with a plasma as its core [6].

The magnetic permeability can be considered to be the parameter determining the process of power transmission from the antenna to the discharge area, because its magnitude defines the plasma resistance and inductance. Such an approach, where instead of two variables, the plasma resistance and the inductance, causing measuring ambiguity, only  $\mu$  is involved, can be useful.

The inductance is calculated by using indirect methods, proceeding from the electromagnetic field distribution inside ICP source in terms of Maxwell equations. The first model was proposed by Ventzek and Kushner [7]. However, this model can't be applied at low pressures when the electron distribution along the radial coordinate tends to be uniform due to the high mobility. Nevertheless, at a pressure of  $10^{-3}$  Torr, a charge distribution peak is usually observed. Still, difficulties in performing electron current measurements by using contact methods (first of all, due to plasma perturbation) make the model of Ventzek and Kushner hardly applicable in practical work. As for the plasma resistance, existing measuring procedures require some essential approximations. It is important at present to estimate the magnitude of the plasmas magnetic permeability averaged over the period of an RF current oscillation by using the inductance coils when the operating frequency of

---

\*E-mail: oleksiy@skku.edu

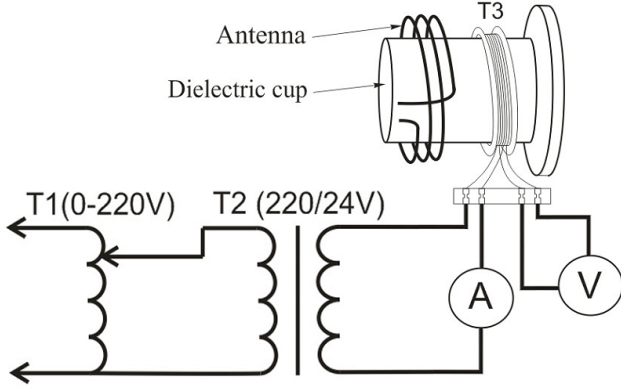


Fig. 1. Solenoid-type inductive system with measuring transformer T3.

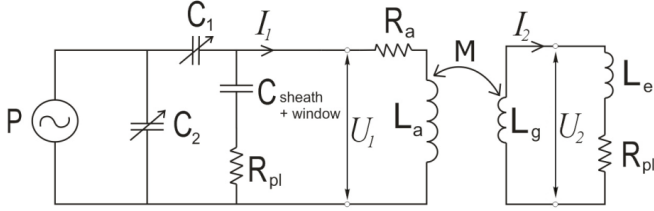


Fig. 2. Equivalent electric circuit for the RF circuit. Here, the electromagnetic interaction is realized by means of inductive coupling between the antenna coil and the plasma.

measuring device is significantly lower than the plasma's oscillation frequency.

## II. EXPERIMENT AND DISCUSSION

Fig. 1 shows the scheme of the experiment with an equivalent electrical circuit. When the source of an AC current with a 60-Hz frequency, generated by transformers T1 and T2, is connected to the primary coil of the transformer T3, the current in it causes a magnetic flux inside the measuring coil. Part of this flux ties the secondary coil and is responsible for EMF generation. Under the influence of an electromotive force a current appears in the load circuit producing magnetic flux inside the secondary coil. The flux generated by the secondary coil's current ties, according to the Lenz's rule, primary coil, aiming in the opposite direction relative to the primary coil's flux, where gives rise to an EMF and a current in the secondary coil of the measuring transformer. The primary and the secondary coils are considered to be inductively coupled with oppositely directed internal magnetic fluxes.

In order to calculate the antenna coil's impedance, we used equivalent circuits [8–12], where the electromagnetic connection with the plasma was replaced by electrical coupling. The components of the circuits are arranged in such a way, that their currents and voltages

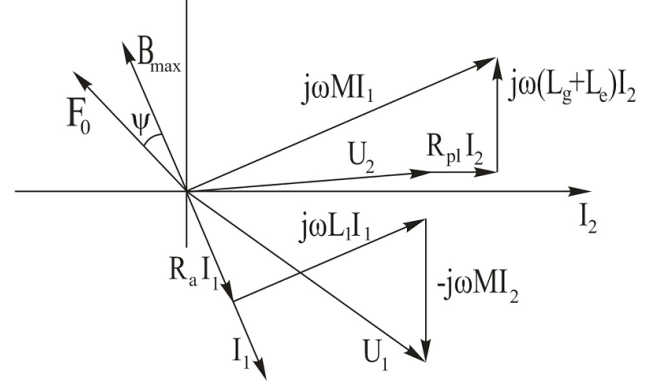


Fig. 3. Vector diagrams for the currents generated during the process of inductive coupling.

are described by the same equations as would be used for real electrical lines.

The equivalent electric circuit of the antenna-plasma system, for which an electromagnetic oscillation takes place during resonance, is shown in Fig. 2.

The impedance-matching network contains variable capacitors  $C_1$  and  $C_2$ . The capacitance of the space-charge region and of the window,  $C_{sheath+window}$ , should also be considered because during discharge formation, the complex resistance of  $C_{sheath+window} - R_{pl}$  is comparable to plasma's circuit resistance, as shown in the right part of Fig. 2.

Fig. 3 shows a vector diagram for the currents and the voltages observed in the plasma and in the oscillation loop in a rectangular coordinate system. The X-axis coincides with the vector of the secondary current  $I_2$ , which is formed mainly by plasma electrons having a velocity in the azimuthal direction in a cylindrical coordinate system related to the source's central line [13]. The vector of the magnetodynamic force (not shown on the picture) is parallel to the current  $I_2$ . The vector of internal voltage  $U_2$  is attached to the origin of the coordinate system; its end coincides with the beginning of the vector  $R_{pl}I_2$ . From the end of the vector  $R_{pl}I_2$  at a right angle to it, the inductive voltage drop on the secondary coil,  $j\omega(L_g + L_e)I_2$ , is plotted. The sum of these vectors determines the magnitude of the mutual inductance  $j\omega M$ :

$$j\omega M = \sqrt{(U_{\parallel} + R_{pl}I_2)^2 + (U_{2\perp} + \omega(L_g + L_e)I_2)^2}, \quad (1)$$

Here  $U_{2\parallel}$  and  $U_{2\perp}$  are projections of the vector  $U_2$ .

The phase shift between the vector of mutual inductance and the plasma's secondary electron current can be estimated from the formula

$$\alpha = \arctg \frac{U_{2\perp} + \omega(L_g + L_e)I_2}{U_{\parallel} + R_{pl}I_2}. \quad (2)$$

The magnetic flux vector is inclined 90 degrees with respect to its electromotive force. The vector of the magnetic induction  $B$  has the same direction as the magnetic

flux  $\Phi_0$ , and its magnitude can be found by measuring the antenna voltage:

$$B(t) = \frac{U_m}{SN\omega} \cos(\omega t) = \frac{\sqrt{2}U}{SN\omega} \cos(\omega t)$$

Thus its maximum value is

$$B_{max} = \frac{\sqrt{2}U}{SN\omega}, \quad (3)$$

where  $N$  is the number of antenna turns,  $S$  is the reactor cross-section, and  $\omega$  is the operating frequency. The vector of the full magnetodynamic force of the magnetization  $F_0$  leads to the phase vectors  $\Phi_0$  and  $B_{max}$  with an angle of loss  $\psi$ , which characterizes the ratio between the resistive part,  $F_{0a}$ , of the magnetodynamic force  $F_0$  and the inductive force  $F_{0i}$ . Since the inductances  $L_a$  and  $L_g$  are coupled and oppositely powered, from Kirchhoff's equations for these circuits, the following set of equation arises:

$$\begin{cases} U_1 = I_1 R_a + j I_1 \omega L_a - j \omega M I_2 \\ j \omega M I_1 = I_2 j \omega (L_g + L_e) + I_2 R_a \end{cases} \quad (4)$$

If the variable  $I_2$  is eliminated from Eq. (4), it is not difficult to find the input antenna's impedance, which defines the power transferred from the RF generator by means of the electromagnetic radiation:

$$Z_a = \frac{U_1}{I_1} = R_a + \frac{\omega^2 M^2 R_{pl}}{R_{pl}^2 + \omega^2 (L_g + L_e)^2} + j \left( \omega L_a - \frac{\omega^2 M^2 (L_g + L_e)}{R_{pl}^2 + \omega^2 (L_g + L_e)^2} \right),$$

which can be rewritten in the following form:

$$Z_a = R_a + j \omega L_a + \frac{(\omega M)^2}{R_{pl} + j \omega (L_e + L_g)} = Z_{a0} + Z_{pl},$$

where the antenna's input impedance is represented by the sum of two components: the complex resistance of antenna itself in a nonperturbed state  $Z_{a0}$  and the resistance  $Z_{pl}$  contributed by the plasma to the primary antenna's coil by means of inductive coupling.

As Ref. 14 shows, the plasma's inductance and the active part of the resistance is determined by the skin depth at which the electromagnetic energy from the antenna can be effectively transferred to the discharge region, which is given by the formula

$$\delta_s = \left( \frac{2}{\mu \omega \sigma} \right)^{\frac{1}{2}}. \quad (5)$$

Here,  $\mu$  is the plasma's magnetic permeability,  $\sigma$  is the conductivity, and  $\omega$  is the generator's operating frequency. For calculating the numerical value of the plasma conductivity  $\sigma$ , we employed methods based on differential measurements obtained by using a Langmuir probe [7,15].

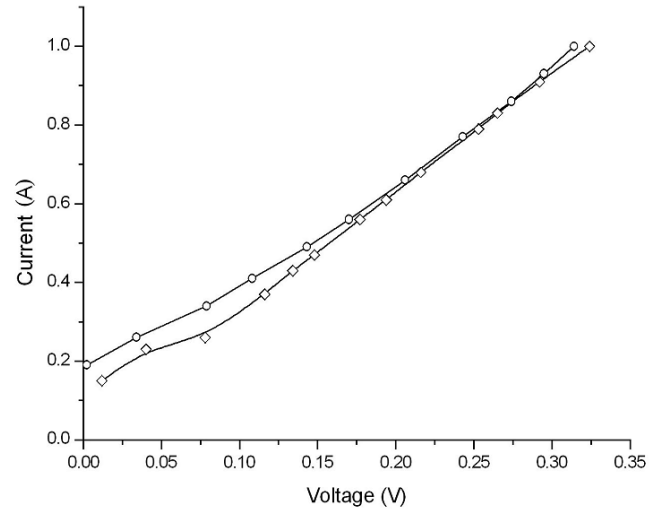


Fig. 4. Volt-ampere curve of the measuring transformer. The gas flow rate was equal to 20 sccm, and the pressure in the chamber was  $2 \times 10^{-4}$  Torr. The upper curve was obtained for a 180-Watt plasma, and the bottom curve for a 200-Watt plasma.

The measurements started from a small magnetization current, which was gradually increased to the saturation of the magnitude of the magnetic permeability. The volt-ampere characteristics of the measuring transformer are shown in Fig. 4. As the graph shows, an almost linear dependence of the magnetizing current on the magnitude of EMF generated at the ends of the secondary coil was observed after the magnetizing current was increased to 0.4 A, which proved that the value of the plasma magnetization was far from saturation; consequently, energy dissipation to the discharge area was not large. This is easy to explain by the fact that the frequency and the amplitude of alternating voltage, generated at both coils of the transformer T3 are significantly lower than the frequency and the voltage of the RF source used for plasma generation and maintenance. Thus, a measuring transformer can be employed as an analyzing instrument for measuring the nonlinear plasma characteristics averaged over a period of the RF oscillation.

Considering the magnetizing current versus self-inductance voltage curve for the magnetic inductance of the transformer T3, we found the magnetic field to be

$$H = Ni \left[ \frac{1}{(L^2 + D^2)^{\frac{1}{2}}} \right] = \frac{\sqrt{2}Ni}{l_c}. \quad (6)$$

Here,  $l_c$  represents the mean magnetic path,  $w$  is the number of turns of the magnetizing coil, and  $L$  and  $D$  are the measured transformer thickness and diameter, respectively.

The magnetic field is determined by Eq. (3), which was also used for plotting the vector diagram of the induction coupling in the plasma. In our case,  $S$  includes the cross section of the reactor volume at the point where

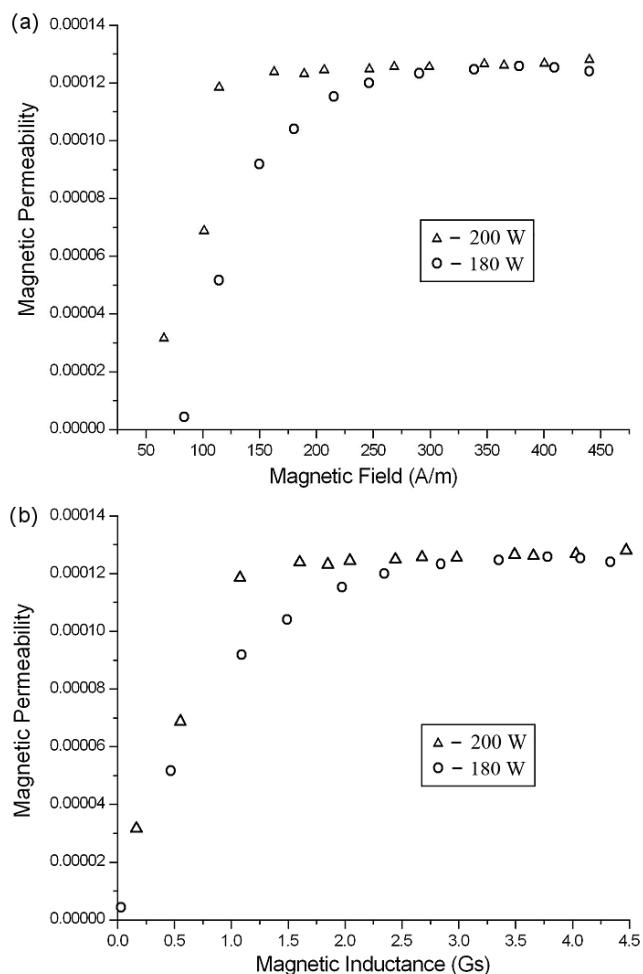


Fig. 5. Plasma magnetic permeability against the (a) magnetic field and the (b) magnetic inductance. The result is shown for 180 (circle)- and 200 (triangle)-Watt argon-plasma generation.

permeability is measured and the cross section of the dielectric window separating the plasma from the measuring transformer. The expression for magnetic permeability includes both the magnetic inductance and the magnetic field:

$$\mu = \frac{B_m}{\mu_0 \cdot H_m}. \quad (7)$$

In Figs. 5(a) and 5(b), the dependences of the magnetic permeability on the magnetic field and the inductance are shown for 180- and 200-watt Ar plasmas generated at a working pressure of  $2 \times 10^{-4}$  Torr. Their behaviors differ only slightly from each other due to the almost linear dependence of magnetizing current on the generated voltage. As Fig. 5 shows, when the field is low, the magnetic permeability grows linearly in the discharge region where the measuring transformer is placed, which is caused by the magnetization of the medium. When the field magnitude reached 250 A/m and the magnetic

inductance reached 2.4 Gs, permeability saturation was observed. It is noteworthy that the plasma was not affected significantly by the probe because the magnitudes of the tuning capacitors remained stable in the auto tuning mode in spite of their sensitivity. Therefore, the antenna impedance was also constant.

### III. CONCLUSION

A model of the electromagnetic oscillations in an ICP source was considered by implementing notions of current and voltage vectors. The formula for a complex antenna's impedance was derived. A method for the magnetic permeability measurement is presented. Experimental results showed that during plasma excitation, the magnetic permeability had a non-linear dependence on the magnetic field. Permeability saturation was observed, which determined the limits of effective power transmission from the antenna to the plasma. The permeability demonstrated a strong dependence on the induced power when the magnetic field was low. The parameters of plasma generation were undisturbed during the experiment, which allowed the non-linear plasma characteristics to be measured by using a measuring transformer as a probe.

### ACKNOWLEDGMENTS

This work was supported by the National Program for Tera-level Nanodevices of the Korea Ministry of Science and Technology as one of the 21st Century Frontier Programs.

### REFERENCES

- [1] D. K. Coultas and J. H. Keller, *European Patent Application* 0 379 828 A2 (1989).
- [2] J. D. Jackson *Classical Electrodynamics*, 1st ed. (Wiley, New York, 1965) p. 226; *Classical Thermodynamics*, 2nd ed. (Wiley, New York, 1975), p. 298.
- [3] D. E. Ibbotson, A. D. Johnson, C. P. Chang and J. F. Miner, *Studies of a High Density, Radio Frequency Plasma Source for Polysilicon Gate Etching* (Murry Hill, New Jersey, 1990).
- [4] M. J. Kushner, *J. Appl. Phys.* **53**, 2923 (1982).
- [5] E. S. Aydil and D. J. Economou, *J. Electrochem. Soc.* **139**, 1397 (1992).
- [6] D. B. Ilic, *Rev. Sci. Instrum.* **52**, 1542 (1981).
- [7] P. L. G. Ventzek, R. J. Hockstra and M. J. Kushner, *J. Vac. Sci. Technol. B* **12**, 461 (1994).
- [8] N. S. Yoon, S. S. Kim, C. S. Chang and Duk-In Choi, *J. Korean Phys. Soc.* **28**, 172 (1995).
- [9] J. H. Keller, J. C. Forster and M. S. Barnes, *J. Vac. Sci. Technol. A* **11**, 2487 (1993).

- [10] R. B. Piejak, V. A. Godyak and B. M. Alexandrovich, *Plasma Sources Technol.* **1**, 179 (1993).
- [11] J. W. Denneman, *J. Appl. Phys.* **23**, 293 (1990).
- [12] H. U. Eckert, *J. Appl. Phys.* **33**, 2780 (1962).
- [13] V. V. Afanasiev, N. M. Adoniev and V. M. Kibel, *Current transformers*, 2nd ed. (Russia, Energoatomizdat, 1989), p. 18.
- [14] O. A. Popov, *High Dens. Plasma Sourc.* (Park Ridge, New Jersey, 1995), p. 85.
- [15] J. Hopwood, C. R. Guarnieri, S. J. Whitehair and J. J. Cuomo, *J. Vac. Sci. Technol. A* **11**, 152 (1993).